

Mechanism of Chronic Stress-induced Reduced Atherosclerotic Medial Area and Increased Plaque Instability in Rabbit Models of Chronic Stress

Ze-Mou Yu¹, Xiao-Tao Deng², Ruo-Mei Qi³, Lu-Yan Xiao⁴, Chong-Qing Yang⁵, Tao Gong¹

¹Department of Neurology, Beijing Hospital, National Center of Gerontology, Beijing 100730, China

²Department of Radiology, Beijing Hospital, National Center of Gerontology, Beijing 100730, China

³The MOH Key Laboratory of Geriatrics, Beijing Hospital, National Center of Gerontology, Beijing 100730, China

⁴Department of Laboratory, Beijing Hospital, National Center of Gerontology, Beijing 100730, China

⁵Department of Pathology, Beijing Hospital, National Center of Gerontology, Beijing 100730, China

Abstract

Background: Chronic stress contributes to increased risks of atherosclerotic diseases including heart disease, stroke, and transient ischemic attack. However, its underline mechanisms are poorly understood. This study aimed to elucidate the mechanism via which chronic stress exerts its effect on atherosclerosis (AS).

Methods: Fifty male New Zealand white rabbits were used. Aortic balloon-injury model was applied. Both social stress and physical stress methods were adopted to establish chronic stress models. The lumen stenotic degree, intimal and medial areas, maximum fibrous cap thickness, and plaque contents were measured with histological sections. Proteomic methods were applied to detect protein changes in abdominal aortas to identify the specialized mediators. Real-time reverse transcription-polymerase chain reaction was used for further verification and investigation.

Results: The stress rabbits exhibited lower body weight, worse fur state, more inactivity behavior, and higher serum cortisol level. Chronic stress was significantly associated with the decreased medial area and increased plaque instability, which was manifested by thinner fibrous caps, larger lipid cores, more macrophages, and new vessels but fewer smooth muscle cells and elastic fibers. After chronic stress, the apoptosis-related genes *UBE2K*, *BAX*, *FAS*, *Caspase 3*, *Caspase 9*, and *P53* were upregulated, and *BCL-2/BAX* was down-regulated; the angiogenesis-related genes *ANG* and *VEGF-A* were also highly expressed in atherosclerotic arteries.

Conclusions: Rabbit models of chronic stress were successfully established by applying both social stress and physical stress for 8 weeks. Chronic stress can reduce AS tunica media and accelerate plaque instability by promoting apoptosis and neovascularization.

Key words: Atherosclerosis; Chronic Stress; Plaque Stability; Rabbit Model; Tunica Media

INTRODUCTION

Research has shown chronic stress may promote the development of atherosclerosis (AS) and increase the risk of cardiovascular events and incident stroke.^[1,2] Meanwhile, a positive and stable social environment may slow down the progression of AS.^[3] A correlation among glucocorticoid, chronic inflammation, and chronic-stress-induced AS has been documented.^[4,5] However, most of these experiments used mice (especially apoE^{-/-}-mice) as animal models and mainly focused on the effects of stress on total lesion areas rather than on atherosclerotic vascular wall or plaque stability.^[6]

In human beings, the unstable atherosclerotic plaques are most responsible for the risk of acute atherothrombotic events.^[7] To explore the effects of chronic stress on plaque stability, animal model with the same human plaque features

Address for correspondence: Dr. Tao Gong,
Department of Neurology, Beijing Hospital, National Center of
Gerontology, Beijing 100730, China
E-Mail: gb20598@sina.com

This is an open access article distributed under the terms of the Creative Commons Attribution-NonCommercial-ShareAlike 3.0 License, which allows others to remix, tweak, and build upon the work non-commercially, as long as the author is credited and the new creations are licensed under the identical terms.

For reprints contact: reprints@medknow.com

© 2018 Chinese Medical Journal | Produced by Wolters Kluwer - Medknow

Received: 03-08-2017 **Edited by:** Yi Cui

How to cite this article: Yu ZM, Deng XT, Qi RM, Xiao LY, Yang CQ, Gong T. Mechanism of Chronic Stress-induced Reduced Atherosclerotic Medial Area and Increased Plaque Instability in Rabbit Models of Chronic Stress. *Chin Med J* 2018;131:161-70.

Access this article online

Quick Response Code:



Website:
www.cmj.org

DOI:
10.4103/0366-6999.222322

should be used. Since rabbits are feasible for research on AS in terms of lipid metabolism^[8] and closely resembling plaque,^[9] we planned to establish a chronic stress model in New Zealand white rabbits.

The effect of chronic stress on AS involves multiple and complex pathways. Therefore, identification of novel targets requires a further understanding of the differentially expressed proteins in the atherosclerotic artery wall with or without chronic stress. The changed proteins may be linked with chronic-stress-induced structural changes in arterial wall and advanced vulnerable lesions.

Accordingly, we aimed to investigate the effects of chronic stress on abdominal AS and to explain the possible mechanisms in rabbit chronic stress models. The impacts of chronic stress including social stress and physical stress were assessed on behavioral, neuroendocrine, lipid metabolism, inflammation, and AS plaque characteristics. Moreover, given that the chronic stress has been shown to affect AS progress, we also used proteomics for further mechanism study.

METHODS

Animals, groups, and diets

The experimental protocol was approved by the Animal Care and Use Committee of the Institute of Laboratory Animal Sciences, Chinese Academy of Medical Sciences and Peking Union Medical College. All efforts were made to reduce pain and minimize suffering during the procedures.

Fifty male New Zealand white rabbits (2.5 months old, about 2.5 kg) were obtained from the institute. All animals were housed in individual cages (50 cm × 40 cm × 40 cm) and maintained in standard conditions of temperature (22 ± 1°C), relative humidity (60%), and a 12-h light/dark cycle (lights on at 07:00 a.m.).

After one week of acclimation, the rabbits were randomly divided into four groups: control group (Control group, *n* = 10), fed with standard rabbit chow (0% cholesterol); chronic stress group (Chronic Stress group, *n* = 10), fed with standard diet and given chronic stress for 8 weeks; balloon-injury operation plus high fat diet (HFD) model group (Operation + HFD group, *n* = 15), in which balloon-injury operation was combined with a high-fat diet (6% bean oil and 1% cholesterol) for 8 weeks; and

balloon-injury operation plus a high-fat diet plus chronic stress group (Operation + HFD + Chronic Stress group, *n* = 15), receiving operation, high-fat diet, and 8-week chronic stress. Water was ad libitum, and cabbages were provided once a week.

Aortic balloon-injury model

After the rabbit was anesthetized with sodium pentobarbital (30 mg/kg) through marginal ear vein, a longitudinal incision was performed in the right groin, and the femoral artery was isolated. A 3 mm × 20 mm balloon catheter was advanced into the abdominal artery, inflated with 10 atm, and then, gently denuded three times. The procedures were performed under sterile conditions. Before being placed in their cages, the animals were allowed to recover under observation. In the first five days after surgery, benzylpenicillin sodium was administered by intramuscular injection at a dose of 40,000 U per day. The animals were provided with a normal chow diet for 4 weeks, followed by a high-fat diet for 8 weeks.^[9]

Chronic stress procedures and assessments of chronic stress model

Stress is defined as a threatened state provoked by physiologic, psychological, or environmental stressors.^[10] As there is no standard stress procedure for rabbits, we adopted both social stress (referred to as unstable social environment model) and physiologic stress (referred to as rat chronic unpredicted mild stress model, CUMS) methods [Table 1]. These two stress groups (Chronic Stress group and Operation + HFD + Chronic Stress group) were assigned in a separate room to avoid interfering the non-stress groups (Control group and Operation + HFD group). To reduce gastrointestinal injuries, stress manipulation was conducted after feeding, at least half an hour later.

Social stress procedures: animals were paired together in one cage for 4 hours per day and the pairings were exchanged within the own groups every week, forcing rabbits to continually reestablish social relationships.^[3] The time that rabbits in other cage (as intruder) and in home cage during the entire experiments should be balanced.

Physical stress procedures: continuous overnight illumination, 2 h of white noise (a tone of 80 dB), and 2 h of high-intensity stroboscopic illumination (300 flashes/min) were selected separately at different days. To reduce habituation, one-foot

Table 1: Chronic stress procedures

Methods	Time					
	Monday	Tuesday	Wednesday	Thursday	Friday	Saturday
Social stress	4 h	4 h	4 h	4 h	4 h	4 h
Physical stress						
Overnight illumination	12 h	–	–	–	–	–
White noise (80 db)	–	2 h	–	–	–	–
Stroboscopic illumination	–	–	2 h	–	–	–
Foot shock (1 mA)	–	–	–	5 times	–	–

–: Not available.

shock (1mA) was added (several seconds/time, five times in total).^[11] The stress regime was started at the end of week 4 and lasted for 8 weeks.

The rabbits were carefully inspected after stress exposure. The fur scoring was recorded to reflect the basic health status (referred to as the standard of mouse).^[12] To obtain the information on the impact of the stressors on animal behavior in natural state, all rabbits were recorded for 10 min on video, between 8:00 a.m. and 9:00 a.m. before the rabbits began eating. The video was recorded 3–4 times every week. The individual behavioral assessment of the same group was summed to provide a total score of each 4-week stress period.

Fur score: 1 point represents clean, shiny, and tidy fur; 2 points represent dull and irregular fur, with a few minor wounds; 3 points represent less hair fur, more marked with minor wounds; and 4 points represent lack of hair, ruffled fur, with several minor wounds. Rabbits with obvious wounding were excluded from the study.

Behavior score: it was observed that rabbit behaviors were mainly classified into inactivity, locomotor, grooming, and drinking. Inactivity was defined as rabbits sitting or huddling quietly in the cage. Locomotor behaviors comprised of cage exploration, walking, stretching out, and reacting to the other rabbits in the same room. Grooming behavior included licking their paws and using their paws to wipe and wash their face, ears, trunk, or hindquarters.^[13] The behavioral activity of the 4 categories for each rabbit was scored as the percentage of 10-min observation period. The total percentage time in each group was calculated every 4 weeks after stress exposure (at week 8 and 12).

Blood sampling and biochemical assays

Rabbit blood samples were obtained from the central ear artery between 7:00 a.m. and 9:00 a.m. every 4 weeks, after 12 h of fasting. The serum samples separated by centrifugation at 4°C were stored in aliquots at –80°C.

The concentrations of total cholesterol (TC), triglyceride (TG), low-density lipoprotein (LDL), and high-density lipoprotein (HDL) were measured by an automated analyzer (Beckman, USA). High-sensitivity C-reactive protein (hs-CRP) was measured by enhanced immunoturbidimetric assay. Cortisol and interleukin-6 (IL-6) were measured by commercially available enzyme-linked immunosorbent assay (ELISA) kits (R and D Systems, Minneapolis, MN, USA).

Histomorphometric methods and measures

After being euthanized with ketamine hydrochloride, the whole abdominal aorta was removed and then evenly cut into four segments. Two of these parts (near iliac artery) were embedded in Tissue-Tek OCT compound (Sakura, Tokyo, Japan) for frozen sectioning and the others were snap-frozen in liquid nitrogen for proteomic analysis. The bilateral adrenal glands were removed and weighed, expressed as a percentage of body weight.

Serial 6- μ m-thick sections were collected on slides and visualized by hematoxylin and eosin (H and E staining),

Oil red O, and Verhoeff–Van Gieson (VVG) staining. Immunohistochemical staining was conducted with primary antibodies, comprising mouse anti-CD68 (ab31630, Abcam), human α -smooth muscle actin (1A4, Sigma), and mouse anti-CD31 (ab199012, Abcam).

After slicing, the remaining embedded vessels (about 3 mm) were placed in normal saline for gross examination using stereoscopic microscope (Axio Zoom V16, ZEISS, Germany). Planimetry was measured on digitized images with $\times 40$ magnification of H & E stained sections. Intimal area was calculated by subtracting the luminal area from the area bounded by internal elastic lamina, and medial area was calculated by subtracting the area within the internal elastic lamina from the area bounded by external elastic lamina, using ZEN software (ZEISS Microsystems).

The fibrous caps, the lipid contents (determined as red in Oil red O staining), and the amounts of macrophages, smooth muscle cells (SMCs), and new vessels (determined as brown signals) were observed under light microscopy (BX51, OLYMPUS, Japan). IMAGEPRO PLUS was used to quantify maximum fibrous cap thickness, and plaque contents, indicated as ratios (%) of the positive area/intimal area. Elastic fibers were determined as dark violet or black in VVG staining. The thickness of the fibrous cap was measured at the thickest portion of the cap. Mean values were calculated by areas measured on 2 parts (6 replicates for each section) per artery.

Proteomics

To explore the possible mechanisms, we used isobaric tags for relative and absolute quantification (iTRAQ) techniques combined with multidimensional liquid chromatography-tandem mass spectrometry (LC-MS/MS) analysis to perform a quantitative proteomic analysis. Equal quality of abdominal aortic tissues within the same group (Control, Operation + HFD, and Operation + HFD + Chronic Stress groups) were mixed and ground in liquid nitrogen and lysed using protein extraction buffer. iTRAQ (AB Sciex, USA) with different reporter ions were applied as isobaric tags for relative quantification. The LC-MS/MS analysis was carried out using Q Exactive mass spectrometer (Thermo Scientific, USA). Proteome Discoverer software (Thermo Scientific, USA, version 1.4) was used to perform database searching against the NCBI's RefSeq rabbit protein sequence database using the Sequest algorithms.

Real-time reverse transcription-polymerase chain reaction

Total RNA from abdominal aortic tissues was extracted using TRIzol reagent according to standard protocols. Primers are listed in Table 2. Reverse transcription-polymerase chain reaction (RT-PCR) was performed in ABI QuantStudio 7 Flex Real-Time PCR system (Applied Biosystems, Foster City, CA, USA). Actin was used as the internal housekeeping gene. The relative level of the target gene was calculated using the formula of $2^{-\Delta c}$ (average ct of target gene – average ct of housekeeping gene). Then, the target gene levels in

Table 2: Primers for real time PCR

Gene	Forward	Reverse	GenBank number
<i>BAX</i>	5'-TCCTCTCTACTTCGGGACC-3'	5'-AGTAAGAAAAACGCCTGTGTCC-3'	XM_002723696.3
<i>BCL2</i>	5'-TTTTTCAACAGAGCGGTGCG-3'	5'-CGCTCTACCAGAGAACAGGC-3'	XM_008261439.2
<i>UBE2K</i>	5'-TTCCGTCACAGGGGCTATTT-3'	5'-GCATCTTGTGGGTCACTGG-3'	XM_002709395.3
<i>CASP3</i>	5'-GGTAGCGACAGAGTTCGAGT-3'	5'-TGAGAGGGAAGCAGAGTAACAG-3'	XM_008273924.2
<i>CASP9</i>	5'-TGTTTCCGAGCGAGGGATT-3'	5'-CGCAGGAAGGTTTTGGGGTA-3'	XM_008249762.2
<i>p53</i>	5'-ATGCCTACCTCACGGGTCT-3'	5'-AGGGTAGGGAACCAGCACCAT-3'	NM_001082404.1
<i>FAS</i>	5'-CTTTGCACGGGTGTTGGTA-3'	5'-TGGTAGGGAGAGGGGCTTAT-3'	NM_001081995.1
<i>ANG</i>	5'-AGCTCTGTGTGGATCTGACAA-3'	5'-TGCCTGTAGTTTCAGTCCTT-3'	XM_002718039.3
<i>VEGF-A</i>	5'-ATGCGGATCAAACCTCACCA-3'	5'-TTTCGTTTTTGCCCTTGCC-3'	XM_017345155.1
<i>TSP-1</i>	5'-TGGCGGTAGACTAGGGATGT-3'	5'-CCCATCGTTCAGAAGGTGC-3'	XM_002717799.3
<i>ACTIN</i>	5'-TGGCTTAACAGTCCGCCTAG-3'	5'-AGTGCACGTGGACATCCG-3'	NM_001101683.1

PCR: Polymerase chain reaction; BAX: Bcl-2 Associated X Protein; UBE2K: Ubiquitin-conjugating enzyme E2 K; CASP: CysteinyI aspartate specific proteinase 3; ANG: Angiogenin; VEGF-A: Vascular endothelial growth factor-A; TSP-1: Thrombospondin-1.

Operation + HFD and Operation + HFD + Chronic Stress groups were normalized against the Control group.

Statistical analyses

The results are expressed as the mean \pm standard error (SE). Statistical analyses were performed using SPSS 20.0 software (IBM Corp., USA). Statistical significance was determined by Student's *t*-test when two groups were compared. One-factor analysis of variance followed by LSD or Dunnett's test was chosen when four groups were compared. Statistical significance was considered if the $P < 0.05$.

RESULTS

Assessments of chronic stress model

All animals were weighed at week 0 (baseline), week 4, week 8, and week 12. At baseline and week 4, the body weight showed no significant difference among four groups. There was no significant difference in weight gain before and after stress exposure in Operation + HFD + Chronic Stress group, which might be explained by the effect of the operation. However, in Chronic Stress group, the weight gains, during the first and second 4 weeks with stress procedures, were both decreased compared to weight increment without stress ($t = -4.365$, $P = 0.002$; $t = -3.942$, $P = 0.003$). At week 12, the mean animal weight was significantly lower in Operation + HFD + Chronic Stress group than in Operation + HFD group ($F(3, 41) = 1.845$, $P = 0.026$ [Figure 1a]).

A higher fur score reflects worse basic state. At week 8 and week 12, animals exposed to chronic stress got higher fur score than two groups without stress exposure [$P < 0.001$, Figure 1b].

The stress groups developed insignificantly heavier inactivity behavior than the non-stress groups at week 8; however, there was significantly decreased locomotor behavior in Operation + HFD + Chronic Stress group (vs. Operation + HFD group, $F(3, 111) = 6.277$, $P = 0.017$). At week 12, the stress groups developed significantly heavier inactivity behavior than the non-stress groups (Chronic Stress vs. Control; Operation + HFD + Chronic Stress vs.

Operation + HFD; $F(3, 157) = 8.955$, $P = 0.002$, $P = 0.016$). The grooming behavior was decreased in Chronic Stress group ($F(3, 157) = 3.697$, $P = 0.032$). However, it was not significantly increased in Operation + HFD + Chronic Stress group, suggesting that grooming behavior may be too variable to reflect behavioral differences after chronic stress [Figure 1c].

At week 8, Operation + HFD + Chronic Stress group had significantly higher cortisol level than Operation + HFD group ($F(3, 34) = 56.82$, $P = 0.006$); meanwhile, the Chronic Stress group displayed a nonsignificant increase relative to Control group. At week 12, however, the relative elevated cortisol level in stress groups fell a bit, which might reflect partial adaptation to stress [Figure 1d]; in addition, serum cortisol levels were higher in HFD groups, related to hyperlipidemia.

There were no significant differences in adrenal gland weight/body weight between stress groups and nonstress groups [Figure 1e].

Assessment of serum lipid profile

The mean serum TG ($[2.270 \pm 0.186]$ vs. $[1.449 \pm 0.253]$, $t = 2.349$, $P = 0.027$) and LDL ($[20.385 \pm 0.724]$ vs. $[16.799 \pm 1.058]$, $t = 2.831$, $P = 0.009$) levels in Operation + HFD + Chronic Stress group (vs. Operation + HFD group) were elevated at week 8. The mean serum TC ($[43.987 \pm 0.727]$ vs. $[38.086 \pm 2.569]$, $t = 2.210$, $P = 0.037$) and TG ($[5.842 \pm 0.722]$ vs. $[3.858 \pm 0.438]$, $t = 2.349$, $P = 0.027$) levels were significantly elevated in Operation + HFD + Chronic Stress group at week 12. There was no obvious change in HDL. Compared with Control group, the lipid metabolism showed no significant change after 8 weeks of chronic stress exposure in the Chronic Stress group [Figure 2a].

Assessment of serum high-sensitivity C-reactive protein and interleukin-6 levels

It has been demonstrated that many different forms of chronic stress were associated with inflammation.^[14,15] At week 12, the serum CRP and IL-6 concentrations in Operation + HFD + Chronic Stress group were

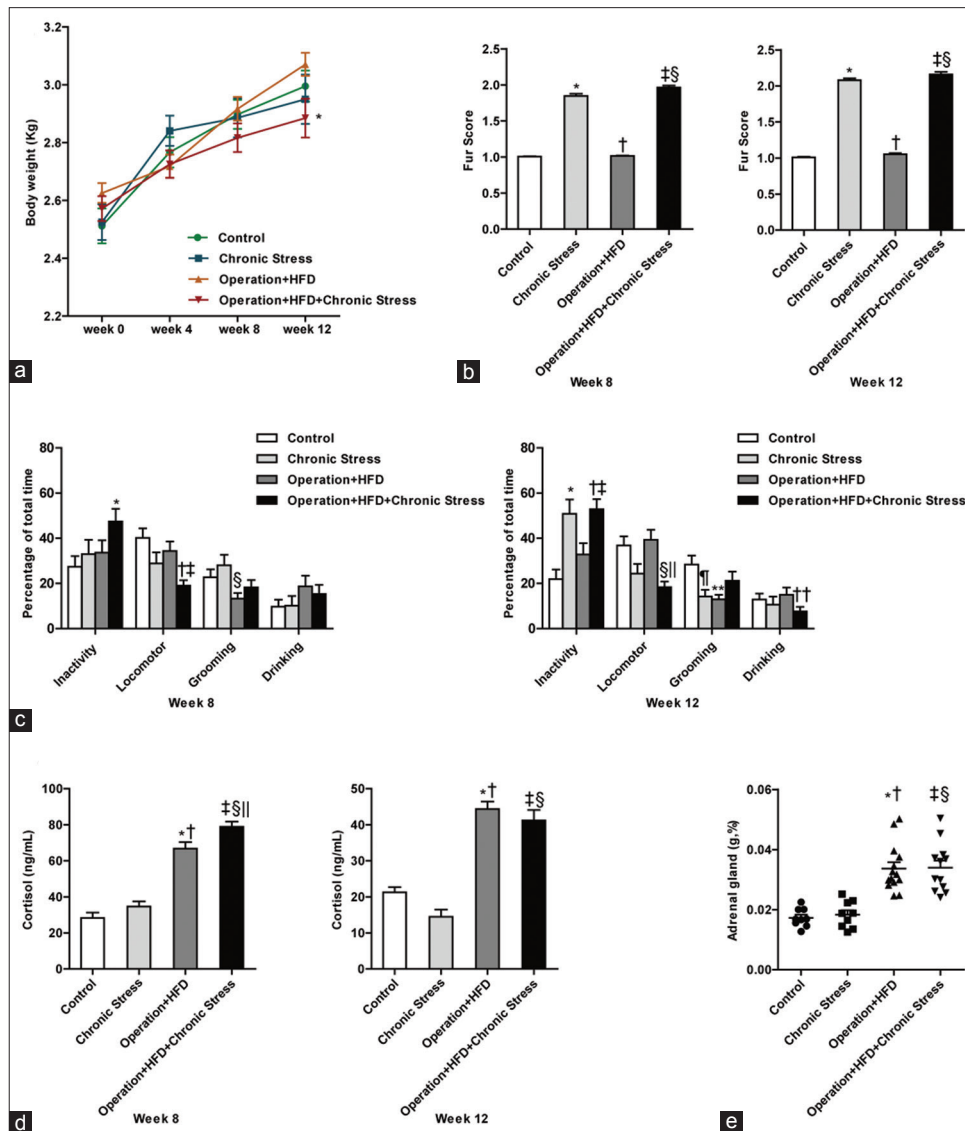


Figure 1: Assessments of chronic stress model. (a) Body weight. * $P < 0.05$ compared with Operation + HFD group. (b) Fur score. At week 8, * $P < 0.001$, † $P < 0.001$ compared with Control group; ‡ $P < 0.001$ compared with Chronic Stress group; § $P < 0.001$ compared with Operation + HFD group. At week 12, * $P < 0.001$, † $P < 0.001$ compared with Control group; ‡ $P < 0.001$ compared with Chronic Stress group; § $P < 0.001$ compared with Operation + HFD group. (c) Behavior assessments. At week 8, * $P < 0.01$, compared with Control group; † $P < 0.001$ compared with Control group; ‡ $P < 0.05$ compared with Operation + HFD group; § $P < 0.01$ compared with Chronic Stress group. At week 12, * $P < 0.01$, † $P < 0.001$ compared with Control group; ‡ $P < 0.05$ compared with Operation + HFD group; § $P < 0.01$ compared with Control group, ¶ $P < 0.01$ compared with Operation + HFD group; †† $P < 0.05$, ** $P < 0.01$ compared with Control group; ‡‡ $P < 0.05$ compared with Operation + HFD group. (d) Serum cortisol. At week 8, * $P < 0.001$, †† $P < 0.001$ compared with Control group, ‡ $P < 0.001$, § $P < 0.01$ compared with Chronic Stress group, ¶ $P < 0.01$ compared with Operation + HFD group. At week 12, * $P < 0.001$, † $P < 0.001$ compared with Control group, ‡ $P < 0.001$, § $P < 0.001$ compared with Chronic Stress group. (e) Adrenal weight/body weight. * $P < 0.001$, †† $P < 0.001$ compared with Control group, ‡ $P < 0.001$, § $P < 0.001$ compared with Chronic Stress group. Data are shown as mean \pm SE. and were analyzed by one-way analysis of variance. (Control group, $n=9$; Chronic Stress group, $n=9$; Operation + HFD group, $n=14$; Operation + HFD + Chronic Stress group, $n=11$).

significantly higher than in Operation + HFD group [Figure 2b and 2c].

Assessment chronic stress on atherosclerosis stenotic degree, intimal area, and medial area

To evaluate structural changes, gross examination of abdominal aorta was performed by stereoscopic microscope. As shown in Figure 2d, operation combined with high-fat food treatment induced obvious AS plaques and artery wall expansion. Further quantitative

analysis of H & E stained sections revealed no remarkable change in the degree of luminal stenosis, expressed as $(1 - \text{lumen area} / [\text{intimal area} + \text{lumen area}] \times 100\%)$ in both stress groups and nonstress groups [Figure 2e and 2f].

The intimal area was also unchanged, which was unexpected [Figure 2g]. However, compared with Operation + HFD group, the Operation + HFD + Chronic Stress group presented significantly decreased medial

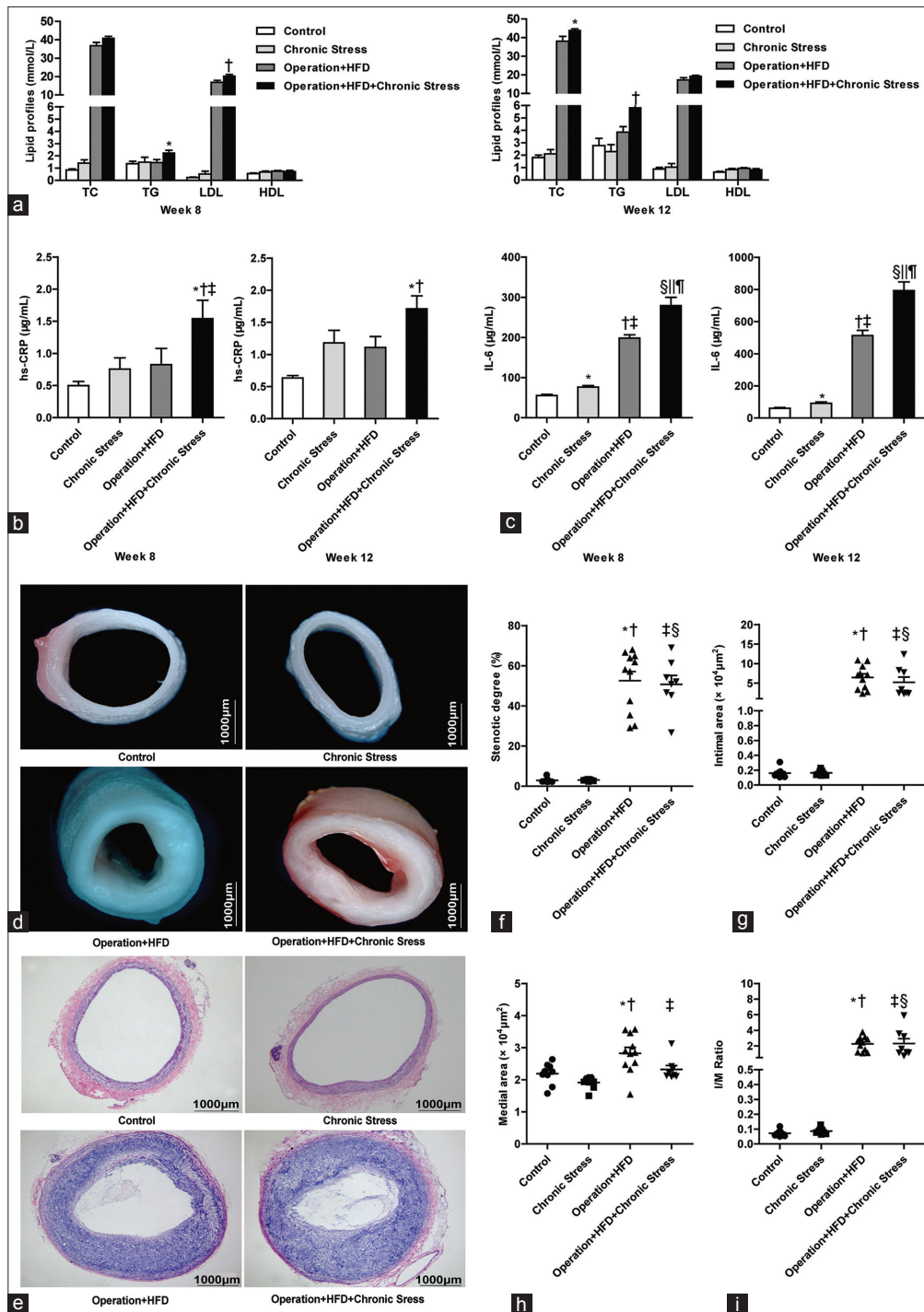


Figure 2: Assessments of chronic stress on lipids, inflammation, stenotic degree, intimal area and medial area. (a) Serum lipid profiles. At week 8, * $P < 0.05$, † $P < 0.01$ compared with Operation + HFD group. At week 12, * $P < 0.05$, † $P < 0.01$ compared with Operation + HFD group. (b) Serum hs-CRP. At week 8, * $P < 0.01$ compared with Control group, † $P < 0.05$ compared with Chronic Stress group, ‡ $P < 0.05$ compared with Operation + HFD group. At week 12, * $P < 0.001$ compared with Control group, † $P < 0.05$ compared with Operation + HFD group. (c) Serum IL-6. At week 8, * $P < 0.01$, † $P < 0.001$, ‡ $P < 0.001$ compared with Control group; § $P < 0.001$, || $P < 0.001$ compared with Chronic Stress group; † $P < 0.05$ compared with Operation+HFD group. At week 12, * $P < 0.05$, † $P < 0.001$, ‡ $P < 0.001$ compared with Control group; § $P < 0.001$, || $P < 0.001$ compared with Chronic Stress group; † $P < 0.01$ compared with Operation+HFD group. (d) Gross examination, ×40. (e) H & E staining, original magnification ×40. (f) Comparison of stenotic degree. * $P < 0.001$, † $P < 0.001$ compared with Control group; ‡ $P < 0.001$, § $P < 0.001$ compared with Chronic Stress group. (g) Comparison of intimal area. * $P < 0.001$, † $P < 0.001$ compared with Control group; ‡ $P < 0.001$, § $P < 0.001$ compared with Chronic Stress group. (h) Comparison of medial area. * $P < 0.01$ compared with Control group, † $P < 0.001$ compared with Chronic Stress group, ‡ $P < 0.05$ compared with Operation + HFD group. (i) Comparison of intima/media area ratio. * $P < 0.001$, † $P < 0.001$ compared with Control group; ‡ $P < 0.001$, § $P < 0.001$ compared with Chronic Stress group. Bars represent SE. Data were analyzed by one-way analysis of variance. (Control group, $n = 9$; Chronic Stress group, $n = 9$; Operation + HFD group, $n = 11$; Operation + HFD + Chronic Stress group, $n = 8$).

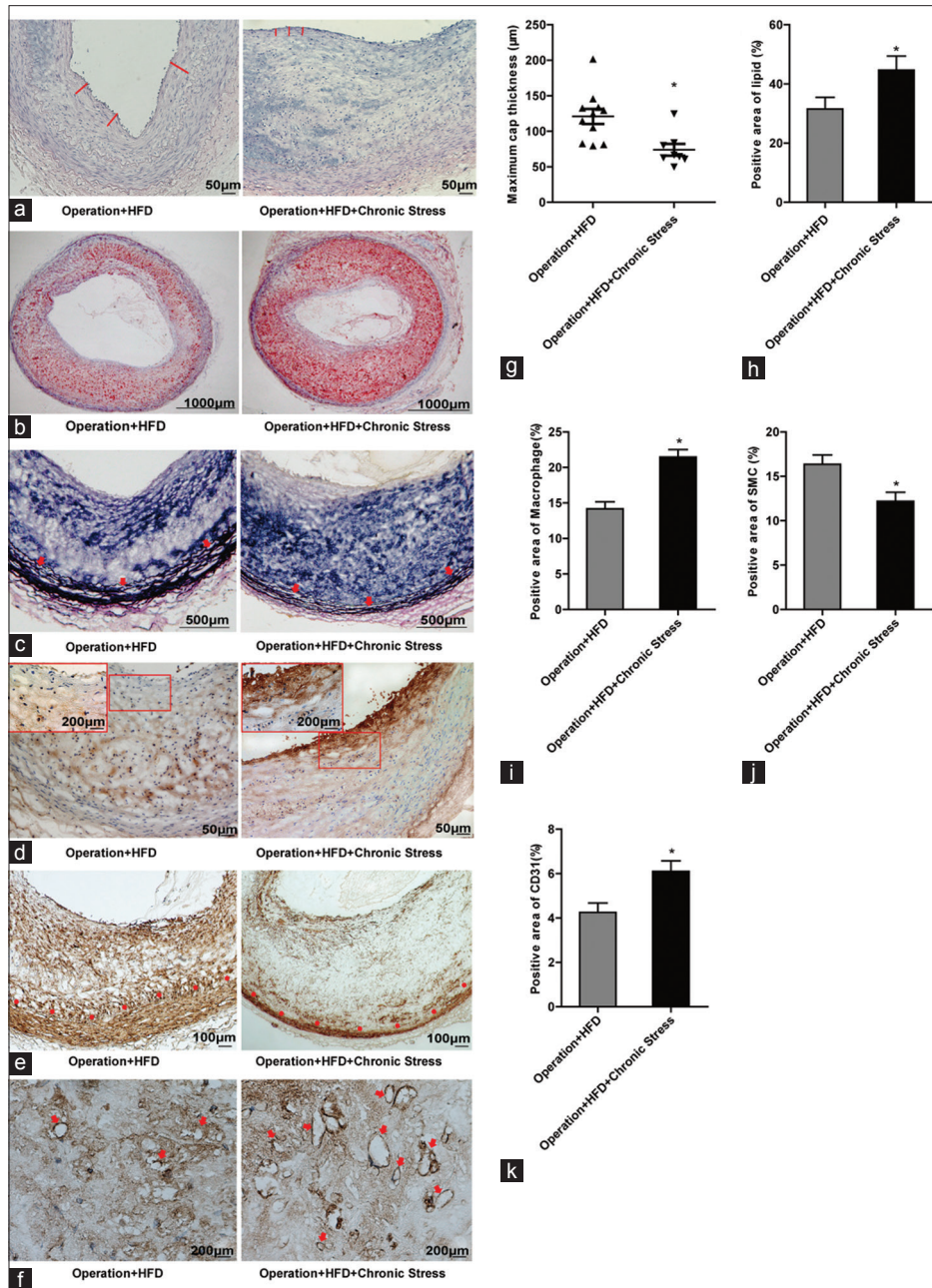


Figure 3: Assessments of chronic stress on plaque stability. (a) H & E staining for fibrous cap (red line), original magnification $\times 100$. (b) Oil red O staining for lipid deposition, original magnification $\times 40$. (c) Verhoeff–Van Gieson staining for elastic fiber (arrowhead, internal elastic lamina), original magnification $\times 100$. (d) Immunostaining for macrophage marker CD68, original magnification $\times 100$. Rectangle represents partial enlarged view, original magnification $\times 400$. (e) Immunostaining for SMC (Dot, internal elastic lamina), original magnification $\times 100$. (f) Immunostaining for new vessels (arrowhead), original magnification $\times 100$. (g) Comparison of the maximum cap thickness, $*P < 0.01$. (h) Quantitative analyses of lipids, $*P < 0.05$. (i) Quantitative analyses of CD68, $*P < 0.001$. (j) Quantitative analyses of SMC, $*P < 0.01$. (k) Quantitative analyses of CD31, $*P < 0.01$. Bars represent SE. Data were analyzed by Student's *t*-test. (Operation + HFD group, $n = 11$; Operation + HFD + Chronic Stress group, $n = 8$).

area [Figure 2h]. The ratio of intimal area/medial area changed insignificantly [Figure 2i].

Effect of chronic stress on atherosclerosis plaque stability

As shown in Figure 3a, the maximum cap thickness was selected from three measurements and calculated. The Operation + HFD + Chronic Stress group exhibited significantly thinner fibrous caps than the Operation + HFD group

([73.974 \pm 8.144] vs. [120.920 \pm 10.692], $t = -3.193$, $P = 0.003$), suggesting plaque vulnerability [Figure 3g].

More lipid-positive areas were found in Operation + HFD + Chronic Stress group than in Operation + HFD group [Figure 3b and 3h].

VVG staining revealed defective internal elastic lamina in Operation + HFD + Chronic Stress group. The elastic fiber

layers were observed to be more substantial and integrated into the tunica media in the Operation + HFD [Figure 3c].

Immunohistochemical staining showed significantly increased amount of macrophage-rich areas in intima, especially near the fibrous caps, in Operation + HFD + Chronic Stress group [Figure 3d and 3i].

Immunohistochemical staining showed significantly decreased amount of SMC-rich area in intima in the Operation + HFD + Chronic Stress group [Figure 3e and 3j]. In addition, the amount of SMCs was reduced in media, indicating that chronic stress accelerated the degrading medial smooth muscle.

Effect of chronic stress on cell apoptosis

In three groups (Control, Operation + HFD, and Operation + HFD + Chronic Stress groups), 444 differentially expressed proteins (≥ 1.5 -fold change) were identified in a total of 3684 proteins. Compared with Operation + HFD group, after stress, there were 63 up-regulated and 29 downregulated proteins [Supplementary Table 1]. The results of pathway analysis of the upregulated proteins are shown in Figure 4a.

From the top 10 pathways, we proposed the apoptosis pathway and lysosome pathway played key roles in stress-mediated medial area reduction. In the high-expression variant proteins, the relative quantity of apoptosis regulator Bcl-2 Associated X Protein (*BAX*) and ubiquitin-conjugating enzyme E2 K (*UBE2K*) was increased by 23.5 folds and 6.0 folds, respectively [Figure 4b and 4c]. Real-time RT-PCR was performed for further verification and investigation. The outcomes showed that, after stress, the apoptosis-related genes *BAX*, *UBE2K*, *FAS*, cysteinyl aspartate-specific proteinase 3 (*Caspase 3*), *Caspase 9*, and *P53* were upregulated by 2.2 folds [$P < 0.001$, Figure 4d], 2.0 folds [$P = 0.002$, Figure 4e], 3.2 folds [$P = 0.011$, Figure 4g], 2.9 folds [$P = 0.040$, Figure 4h], 1.4 folds [$P < 0.001$, Figure 4i], and 1.6 folds [$P < 0.001$, Figure 4j]. *BCL-2/BAX* was downregulated by 0.6 fold [$P = 0.008$, Figure 4f].

Effect of chronic stress on neovascularization

Compared with the Operation + HFD group, the protein angiogenin (*ANG*) in the Operation + HFD + Chronic Stress group was increased by 348.6 folds [Figure 4k]. The expressions of proangiogenic genes *ANG* and vascular endothelial growth factor-A (*VEGF-A*) increased by 2.2 folds each [Figure 4l and 4m]. The expression of thrombospondin-1 (*TSP-1*), an antiangiogenesis gene, showed no significant change [Figure 4n].

Immunohistochemical staining showed that the number of new vessels marked with CD31 in AS plaques was increased after stress exposure [Figure 3f and 3k].

DISCUSSION

Rabbits have rarely been used as an animal model for stress, which is primarily based on rodents. In our current study, we attempted to establish and evaluate a chronic stress model in rabbits and then analyze the effect of chronic stress on AS

in terms of artery wall and plaque stability. Both social and physical stress methods were used during modeling to mimic various stimulations in human beings and reduce adaptation. Physical stress used in our study included noise and strobe light rather than swimming in 4°C cold water or damp sawdust. It was found that exposure to both social and physical stress for 8 weeks in rabbits induce body weight loss, worse fur status, exaggerated inactivity behavior, and increased serum cortisol level. In addition, the results showed that chronic stress promoted lipid metabolism disturbance and inflammation, which was consistent with the previous findings.^[6,16]

Chronic stress may aggravate AS development, as determined by measuring the total lesion areas.^[3] However, few literature has explored the effect of chronic stress on artery structure and plaque stability. We have discovered that chronic stress played a passive role in atherosclerotic media. It is paradoxical that stress may induce media thickening as the sympathetic nervous system can be activated repeatedly on stress exposure. However, in our current study, the vascular SMC layers of atherosclerotic abdominal artery were reduced obviously. There are several reasons as follows: first, compared with abdominal artery, heart ventricle and aortic artery are mainly involved in the increased blood pressure caused by sympathetic overactivation; second, the proliferation and degradation of SMCs are dynamic; and third, chronic stress may prominently promote medial degeneration by accelerating apoptosis.

In our current study, chronic stress increased plaque vulnerability to rupture, characterized with thinner fibrous caps, larger lipid cores, more macrophages and new vessels but less SMCs and elastic fibers. Thus, chronic stress may not induce larger plaque areas but advanced atherosclerotic lesions. Then, how did chronic stress influence AS plaque stability? The level of inflammation and oxidative stress, which can be aggravated by chronic stress, has been proved to be related with the destabilization of atherosclerotic plaque.^[17,18] To further elucidate the pathogenesis, the differentially expressed proteins might provide valuable information. In our current study, we focused on the apoptosis and angiogenesis.

Ubiquitin-proteasome system is the principal degradation route of proteins in eukaryotic cell, playing a crucial role in the regulation of apoptosis.^[19] *BAX* is an important apoptosis regulator, and its excessive expression can adversely affect the protective effect of the *BCL-2*, causing cell apoptosis.^[20] *FAS*, expressed on SMC membrane surface, can combine its ligand FASL to transduce death signal and further activate caspase cascade. *Caspase 9* mainly involves in apoptosis starting. *Caspase 3* is the main effect factor in the process of apoptosis, and its activation signs the irreversible phase of cell apoptosis. *P53* can down-regulate *BCL-2/BAX* to promote apoptosis.^[21] The excessive expressions of genes after stress exposure indicated that chronic stress promoted the apoptosis of AS vascular cells.

The imbalance between proliferation and apoptosis of SMCs is a key factor in occurrence and development of AS.^[22] The increased macrophage apoptosis results in severer plaque

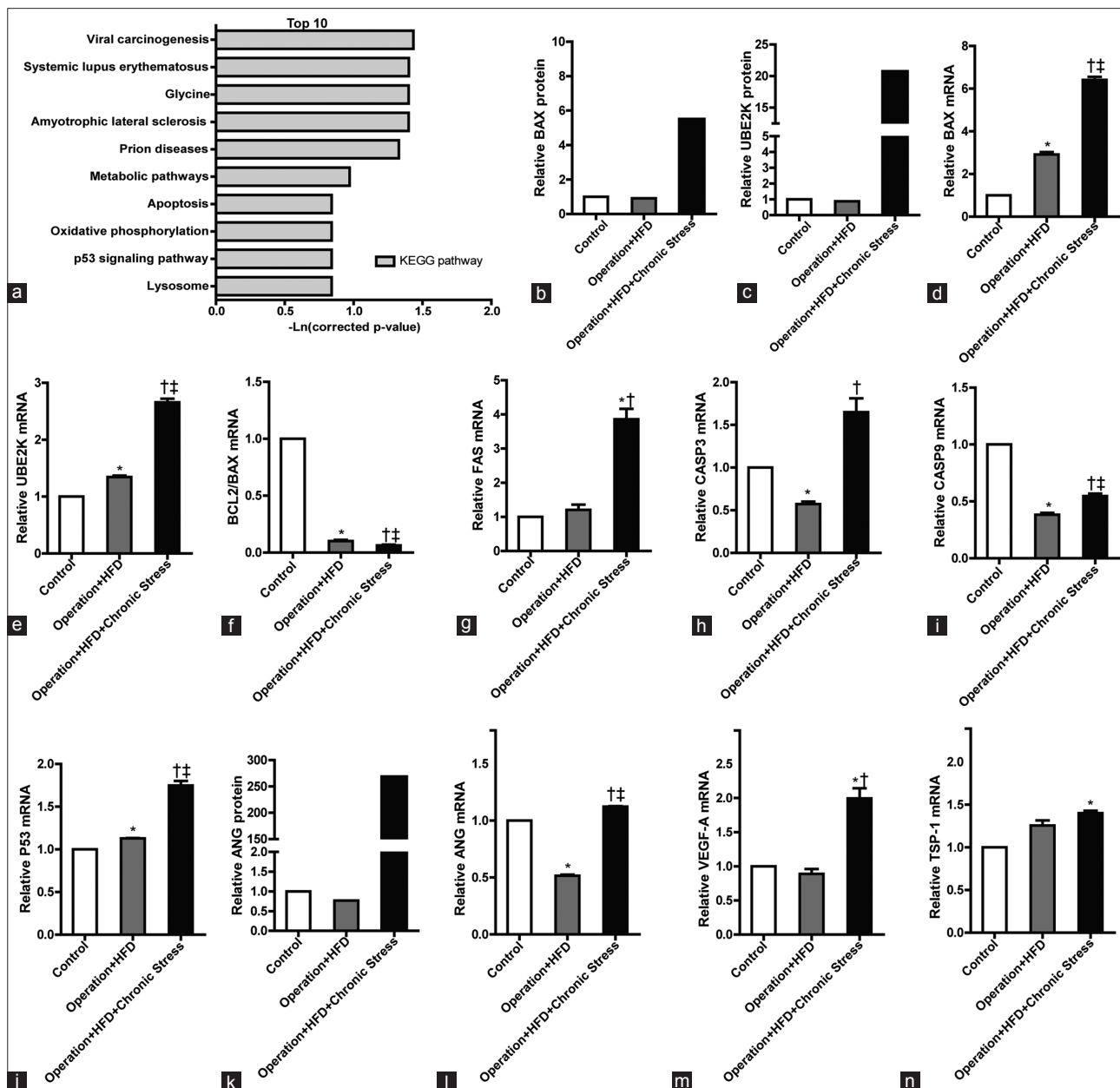


Figure 4: Chronic stress-induced plaque instability associate with increased apoptosis and angiogenesis. (a) Enriched functions associated to the chronic stress to AS (the top 10 pathway). (b) BAX protein level. (c) UBE2K protein level. (d) BAX mRNA expression. * $P < 0.01$, † $P < 0.01$ compared with Control group; ‡ $P < 0.001$ compared with Operation + HFD group. (e) UBE2K mRNA expression. * $P < 0.05$, † $P < 0.01$ compared with Control group; ‡ $P < 0.01$ compared with Operation + HFD group. (f) The ratio of Bcl-2/BAX. * $P < 0.001$, † $P < 0.001$ compared with Control group; ‡ $P < 0.01$ compared with Operation + HFD group. (g) FAS mRNA expression. * $P < 0.05$ compared with Control group; † $P < 0.05$ compared with Operation + HFD group. (h) Caspase3 mRNA expression. * $P < 0.05$ compared with Control group; † $P < 0.05$ compared with Operation + HFD group. (i) Caspase9 mRNA expression. * $P < 0.001$, † $P < 0.001$ compared with Control group; ‡ $P < 0.001$ compared with Operation + HFD group. (j) P53 mRNA expression. * $P < 0.05$, † $P < 0.001$ compared with Control group; ‡ $P < 0.001$ compared with Operation + HFD group. (k) Angiogenin protein level. (l) ANG mRNA expression. * $P < 0.001$, † $P < 0.01$ compared with Control group; ‡ $P < 0.001$ compared with Operation + HFD group. (m) VEGF-A mRNA expression. * $P < 0.001$ compared with Control group; † $P < 0.001$ compared with Operation + HFD group. (n) TSP-1 mRNA expression. * $P < 0.05$ compared with Control group.

burden in more advanced lesions.^[23,24] In this study, the SMC contents in intima and the SMC layers in media were reduced significantly. Thus, stress may promote the apoptosis of SMCs, although further investigation is still required.

Angiogenin, a soluble protein and also one of the most potent angiogenic factors, plays a key role in the growth of new

capillaries.^[25] Several studies have suggested that plasma angiogenin level is remarkably increased in patients with the acute coronary syndrome. Angiogenin may promote AS and lead to the destabilization of atherosclerotic plaque by activating proteases and promoting intralesional angiogenesis.^[25,26] However, the potential effect of chronic stress on angiogenesis has not been validated.

VEGF family is the most commonly known factor in promoting angiogenesis.^[27] VEGF-A, as an important member, may promote intimal hyperplasia and aggravate atherosclerosis by promoting monocyte activation, adhesion, and migration and increasing endothelial cell permeability.^[28] TSP-1 could be expressed in the case of increased angiogenesis, however, the result is not the case, considering that chronic stress compromises the ability of blood vessels to maintain homeostasis. In our current study, the number of new vessels was obviously elevated in the Operation + HFD + Chronic Stress group. Therefore, it is concluded that chronic stress may promote angiogenesis and adversely affect plaque stability.

In conclusions, This study established a chronic stress model in rabbits and then concluded that chronic stress-induced atherosclerotic media reduction and destabilized atherosclerotic lesions, probably by promoting SMCs apoptosis and angiogenesis in plaques.

Supplementary information is linked to the online version of the paper on the Chinese Medical Journal website.

Financial support and sponsorship

This work was supported by a grant from National Natural Science Foundation of China (No. 31271097).

Conflicts of interest

There are no conflicts of interest.

REFERENCES

1. Everson-Rose SA, Roetker NS, Lutsey PL, Kershaw KN, Longstreth WT Jr., Sacco RL, *et al*. Chronic stress, depressive symptoms, anger, hostility, and risk of stroke and transient ischemic attack in the multi-ethnic study of atherosclerosis. *Stroke* 2014;45:2318-23. doi: 10.1161/STROKEAHA.114.004815.
2. Henderson KM, Clark CJ, Lewis TT, Aggarwal NT, Beck T, Guo H, *et al*. Psychosocial distress and stroke risk in older adults. *Stroke* 2013;44:367-72. doi: 10.1161/STROKEAHA.112.679159.
3. McCabe PM, Gonzales JA, Zaias J, Szeto A, Kumar M, Herron AJ, *et al*. Social environment influences the progression of atherosclerosis in the watanabe heritable hyperlipidemic rabbit. *Circulation* 2002;105:354-9.
4. Tang YL, Jiang JH, Wang S, Liu Z, Tang XQ, Peng J, *et al*. Tlr4/nf-kb signaling contributes to chronic unpredictable mild stress-induced atherosclerosis in apoE^{-/-}mice. *PLoS One* 2015;10:e0123685. doi: 10.1371/journal.pone.0123685.
5. Wang S, Xiaoling G, Pingting L, Shuqiang L, Yuaner Z. Chronic unpredictable mild stress combined with a high-fat diets aggravates atherosclerosis in rats. *Lipids Health Dis* 2014;13:77. doi: 10.1186/1476-511X-13-77.
6. Tang YL, Jiang JH, Wang S, Liu Z, Tang XQ, Peng J, *et al*. TLR4/NF-κB signaling contributes to chronic unpredictable mild stress-induced atherosclerosis in apoE^{-/-}mice. *PLoS One* 2015;10:e0123685. doi: 10.1371/journal.pone.0123685.
7. Fredman G, Hellmann J, Proto JD, Kuriakose G, Colas RA, Dorweiler B, *et al*. An imbalance between specialized pro-resolving lipid mediators and pro-inflammatory leukotrienes promotes instability of atherosclerotic plaques. *Nat Commun* 2016;7:12859. doi: 10.1038/ncomms12859.
8. Fan J, Kitajima S, Watanabe T, Xu J, Zhang J, Liu E, *et al*. Rabbit models for the study of human atherosclerosis: From pathophysiological mechanisms to translational medicine. *Pharmacol Ther* 2015;146:104-19. doi: 10.1016/j.pharmthera.2014.09.009.
9. Okabe T, Hoshiga M, Negoro N, Nakakoji T, Arishiro K, Ishihara T, *et al*. Rabbit plaque models closely resembling lesions in human coronary artery disease. *Int J Cardiol* 2011;147:271-7. doi: 10.1016/j.ijcard.2009.09.528.
10. Black PH, Garbutt LD. Stress, inflammation and cardiovascular disease. *J Psychosom Res* 2002;52:1-23. doi: 10.1016/S0022-3999(01)00302-6.
11. Rabasa C, Muñoz-Abellán C, Daviu N, Nadal R, Armario A. Repeated exposure to immobilization or two different footshock intensities reveals differential adaptation of the hypothalamic-pituitary-adrenal axis. *Physiol Behav* 2011;103:125-33. doi: 10.1016/j.physbeh.2011.02.022.
12. Savignac HM, Hyland NP, Dinan TG, Cryan JF. The effects of repeated social interaction stress on behavioural and physiological parameters in a stress-sensitive mouse strain. *Behav Brain Res* 2011;216:576-84. doi: 10.1016/j.bbr.2010.08.049.
13. Aloyo VJ, Dave KD. Behavioral response to emotional stress in rabbits: Role of serotonin and serotonin2A receptors. *Behav Pharmacol* 2007;18:651-9. doi: 10.1097/FBP.0b013e3282effc0d.
14. Cohen S, Janicki-Deverts D, Doyle WJ, Miller GE, Frank E, Rabin BS, *et al*. Chronic stress, glucocorticoid receptor resistance, inflammation, and disease risk. *Proc Natl Acad Sci U S A* 2012;109:5995-9. doi: 10.1073/pnas.1118355109.
15. Bernberg E, Ulleryd MA, Johansson ME, Bergström GM. Social disruption stress increases IL-6 levels and accelerates atherosclerosis in apoE^{-/-} mice. *Atherosclerosis* 2012;221:359-65. doi: 10.1016/j.atherosclerosis.2011.11.041.
16. Kiecolt-Glaser JK, Preacher KJ, MacCallum RC, Atkinson C, Malarkey WB, Glaser R, *et al*. Chronic stress and age-related increases in the proinflammatory cytokine IL-6. *Proc Natl Acad Sci U S A* 2003;100:9090-5. doi: 10.1073/pnas.1531903100.
17. Nation DA, Gonzales JA, Mendez AJ, Zaias J, Szeto A, Brooks LG, *et al*. The effect of social environment on markers of vascular oxidative stress and inflammation in the watanabe heritable hyperlipidemic rabbit. *Psychosom Med* 2008;70:269-75. doi: 10.1097/PSY.0b013e3181646753.
18. Legein B, Temmerman L, Biessen EA, Lutgens E. Inflammation and immune system interactions in atherosclerosis. *Cell Mol Life Sci* 2013;70:3847-69. doi: 10.1007/s00018-013-1289-1.
19. Perego P. The ubiquitin proteasome system as a source of drug targets for cancer therapy. *Curr Pharm Des* 2013;19:4024. doi: 10.2174/1381612811319220011.
20. Misao J, Hayakawa Y, Ohno M, Kato S, Fujiwara T, Fujiwara H, *et al*. Expression of bcl-2 protein, an inhibitor of apoptosis, and bax, an accelerator of apoptosis, in ventricular myocytes of human hearts with myocardial infarction. *Circulation* 1996;94:1506-12.
21. Miyashita T, Krajewski S, Krajewska M, Wang HG, Lin HK, Liebermann DA, *et al*. Tumor suppressor p53 is a regulator of bcl-2 and bax gene expression *in vitro* and *in vivo*. *Oncogene* 1994;9:1799-805.
22. Clarke MC, Littlewood TD, Figg N, Maguire JJ, Davenport AP, Goddard M, *et al*. Chronic apoptosis of vascular smooth muscle cells accelerates atherosclerosis and promotes calcification and medial degeneration. *Circ Res* 2008;102:1529-38. doi: 10.1161/CIRCRESAHA.108.175976.
23. Linton MF, Babaev VR, Huang J, Linton EF, Tao H, Yancey PG, *et al*. Macrophage apoptosis and efferocytosis in the pathogenesis of atherosclerosis. *Circ J* 2016;80:2259-68. doi: 10.1253/circj.CJ-16-0924.
24. Gautier EL, Huby T, Witztum JL, Ouzilleau B, Miller ER, Saint-Charles F, *et al*. Macrophage apoptosis exerts divergent effects on atherogenesis as a function of lesion stage. *Circulation* 2009;119:1795-804. doi: 10.1161/CIRCULATIONAHA.108.806158.
25. Kręcki R, Krzemińska-Pakuła M, Drożdż J, Szcześniak P, Peruga JZ, Lipiec P, *et al*. Relationship of serum angiogenin, adiponectin and resistin levels with biochemical risk factors and the angiographic severity of three-vessel coronary disease. *Cardiol J* 2010;17:599-606.
26. Moreno PR, Purushothaman KR, Fuster V, Echeverri D, Trusczynska H, Sharma SK, *et al*. Plaque neovascularization is increased in ruptured atherosclerotic lesions of human aorta: Implications for plaque vulnerability. *Circulation* 2004;110:2032-8. doi: 10.1161/01.CIR.0000143233.87854.23.
27. Leung DW, Cachianes G, Kuang WJ, Goeddel DV, Ferrara N. Vascular endothelial growth factor is a secreted angiogenic mitogen. *Science* 1989;246:1306-9.
28. Bhardwaj S, Roy H, Heikura T, Ylä-Herttuala S. VEGF-A, VEGF-D and VEGF-D (DeltaNDeltaC) induced intimal hyperplasia in carotid arteries. *Eur J Clin Invest* 2005;35:669-76. doi: 10.1111/j.1365-2362.2005.01555.x.

Supplementary Table 1: Proteomics show the differential expression proteins in operation + HFD + chronic stress group when compared with operation + HFD group

Accession	Description	Operation + HFD + chronic stress group/operation + HFD group
291411929	Predicted: ATP synthase subunit g, mitochondrial (<i>O. cuniculus</i>)	4128.734
655889416	Predicted: Glycogen synthase kinase-3 alpha, partial (<i>O. cuniculus</i>)	1159.396
291395631	Predicted: Histone H2B type 1 (<i>O. cuniculus</i>)	1054.544
291409112	Predicted: Erlin-2 (<i>O. cuniculus</i>)	1054.078
655878391	Predicted: 60S ribosomal protein L35 (<i>O. cuniculus</i>)	929.745
655879926	Predicted: Histone-binding protein RBBP4 (<i>O. cuniculus</i>)	916.680
291391146	Predicted: V-type proton ATPase subunit F (<i>O. cuniculus</i>)	829.562
655839882	Predicted: Histone H2B type 1-B (<i>O. cuniculus</i>)	734.800
291390555	Predicted: Heat shock factor-binding protein 1 (<i>O. cuniculus</i>)	608.791
655859728	Predicted: Nebulette isoform X2 (<i>O. cuniculus</i>)	423.510
291404220	Predicted: Eukaryotic translation initiation factor 4E-binding protein 2 (<i>O. cuniculus</i>)	403.829
291403459	Predicted: Angiogenin (<i>O. cuniculus</i>)	348.576
655884244	Predicted: Serum amyloid A-4 protein-like isoform X2 (<i>O. cuniculus</i>)	339.668
655861225	Predicted: Receptor-type tyrosine-protein phosphatase C isoform X5 (<i>O. cuniculus</i>)	301.419
655830476	Predicted: Serine/threonine-protein kinase 38-like isoform X4 (<i>O. cuniculus</i>)	296.165
655846531	Predicted: Chromatin target of PRMT1 protein isoform X5 (<i>O. cuniculus</i>)	234.743
291397378	Predicted: ATP-binding cassette subfamily F member 2 (<i>O. cuniculus</i>)	224.269
291413675	Predicted: Fructosamine-3-kinase (<i>O. cuniculus</i>)	223.281
291396345	Predicted: Ammonium transporter Rh type A (<i>O. cuniculus</i>)	169.990
655859026	Predicted: Low quality protein: Selenide, water dikinase 1 (<i>O. cuniculus</i>)	78.302
655835923	Predicted: Band 4.1-like protein 3 isoform X30 (<i>O. cuniculus</i>)	41.487
291415261	Predicted: Pyridoxal kinase (<i>O. cuniculus</i>)	35.611
291396976	Predicted: Syntaxin-7 (<i>O. cuniculus</i>)	31.425
126722836	Complement component C8 gamma chain precursor (<i>O. cuniculus</i>)	29.150
655854442	Predicted: Low quality protein: Profilin-2 (<i>O. cuniculus</i>)	27.553
291408940	Predicted: Integral membrane protein 2B (<i>O. cuniculus</i>)	27.449
291396339	Predicted: Methylmalonyl-CoA mutase, mitochondrial (<i>O. cuniculus</i>)	26.848
655853086	Predicted: Schwannomin-interacting protein 1 isoform X4 (<i>O. cuniculus</i>)	25.985
291391482	Predicted: Rab3 GTPase-activating protein catalytic subunit isoform X2 (<i>O. cuniculus</i>)	25.936
655903053	Predicted: AH receptor-interacting protein (<i>O. cuniculus</i>)	25.411
291406912	Predicted: Protein phosphatase 1F (<i>O. cuniculus</i>)	25.166
284005108	Inactive rhomboid protein 1 (<i>O. cuniculus</i>)	24.739
291394851	Predicted: 40S ribosomal protein S17 (<i>O. cuniculus</i>)	24.610
291385675	Predicted: Ubiquitin-conjugating enzyme E2 K (<i>O. cuniculus</i>)	23.543
291388964	Predicted: D-tyrosyl-tRNA (Tyr) deacylase 1 (<i>O. cuniculus</i>)	22.811
655871476	Predicted: Membrane primary amine oxidase-like (<i>O. cuniculus</i>)	22.715
655835965	Predicted: EMILIN-2 (<i>O. cuniculus</i>)	22.411
291398138	Predicted: D-3-phosphoglycerate dehydrogenase (<i>O. cuniculus</i>)	22.262
655604166	Predicted: Low quality protein: Cathepsin F (<i>O. cuniculus</i>)	21.431
655869908	Predicted: Ankyrin repeat and FYVE domain-containing protein 1 (<i>O. cuniculus</i>)	21.316
291415948	Predicted: Epiplakin (<i>O. cuniculus</i>)	21.074
291408920	Predicted: Tubulointerstitial nephritis antigen-like (<i>O. cuniculus</i>)	18.701
291394602	Predicted: Peptidyl-prolyl cis-trans isomerase FKBP14 (<i>O. cuniculus</i>)	16.238
655896783	Predicted: Nuclear factor 1 X-type (<i>O. cuniculus</i>)	15.021
291398563	Predicted: Transcription initiation factor IIB (<i>O. cuniculus</i>)	14.417
655838304	Predicted: Endoplasmic reticulum aminopeptidase 1 isoform X2 (<i>O. cuniculus</i>)	14.254
291384137	Predicted: Protein Hikeshi isoform X1 (<i>O. cuniculus</i>)	12.425
291398326	Predicted: Glutathione S-transferase Yb-3 (<i>O. cuniculus</i>)	12.368
291392588	Predicted: WW domain-binding protein 11 (<i>O. cuniculus</i>)	10.834
655715562	Predicted: Receptor-type tyrosine-protein phosphatase alpha (<i>O. cuniculus</i>)	10.586
291398429	Predicted: Lipoamide acyltransferase component of branched-chain alpha-keto acid dehydrogenase complex, mitochondrial (<i>O. cuniculus</i>)	9.410
655828146	Predicted: SEC14 domain and spectrin repeat-containing protein 1 (<i>O. cuniculus</i>)	9.249

Contd...

Supplementary Table 1: Contd...

Accession	Description	Operation + HFD + chronic stress group/operation + HFD group
655875803	Predicted: Low quality protein: Coiled-coil domain-containing protein 22 (<i>O. cuniculus</i>)	8.909
655898897	Predicted: Kynurenine-oxoglutarate transaminase 1 isoform X5 (<i>O. cuniculus</i>)	8.695
655842122	Predicted: Unconventional myosin-VI isoform X5 (<i>O. cuniculus</i>)	8.309
126723431	Niemann-Pick C1 protein precursor (<i>O. cuniculus</i>)	6.097
291414997	Predicted: Apoptosis regulator BAX isoform X2 (<i>O. cuniculus</i>)	6.008
655893680	Predicted: Myelin basic protein (<i>O. cuniculus</i>)	2.772
655603017	Predicted: Low quality protein: Transmembrane protease serine 13-like (<i>O. cuniculus</i>)	2.150
655845739	Predicted: Myelin protein P0 (<i>O. cuniculus</i>)	2.052
655740408	Predicted: Peripherin (<i>O. cuniculus</i>)	1.955
655877309	Predicted: Myelin proteolipid protein isoform X1 (<i>O. cuniculus</i>)	1.674
655881879	gdp	1.605
291408454	Predicted: 26S proteasome non-ATPase regulatory subunit 5 (<i>O. cuniculus</i>)	0.666
291403258	Predicted: Thrombospondin-1 (<i>O. cuniculus</i>)	0.659
655851215	Predicted: ER membrane protein complex subunit 1 isoform X5 (<i>O. cuniculus</i>)	0.654
126723743	Sex hormone-binding globulin precursor (<i>O. cuniculus</i>)	0.647
291405213	Predicted: Platelet glycoprotein Ib alpha chain (<i>O. cuniculus</i>)	0.643
655898355	Predicted: Acidic leucine-rich nuclear phosphoprotein 32 family member A (<i>O. cuniculus</i>)	0.642
655831559	Predicted: Alpha-2-macroglobulin-like isoform X1 (<i>O. cuniculus</i>)	0.636
655850855	Predicted: PITH domain-containing protein 1 (<i>O. cuniculus</i>)	0.630
655897691	Predicted: Low quality protein: Cytohesin-2 (<i>O. cuniculus</i>)	0.628
655835791	Predicted: Ras-related protein Rab-31 (<i>O. cuniculus</i>)	0.626
284005433	Serpin B10 (<i>O. cuniculus</i>)	0.622
126723213	Tartrate-resistant acid phosphatase type 5 precursor (<i>O. cuniculus</i>)	0.621
291389840	Predicted: Glycosyltransferase 8 domain-containing protein 2 isoform X2 (<i>O. cuniculus</i>)	0.618
655854509	Predicted: Platelet glycoprotein V (<i>O. cuniculus</i>)	0.603
291411025	Predicted: Syntaxin-4 (<i>O. cuniculus</i>)	0.603
126723155	Decorin precursor (<i>O. cuniculus</i>)	0.595
655887741	Predicted: Low quality protein: Syntaxin-binding protein 2 (<i>O. cuniculus</i>)	0.589
930841416	Hemoglobin subunit beta-1/2 isoform 1 (<i>O. cuniculus</i>)	0.587
655900718	Predicted: Fermitin family homolog 3 (<i>O. cuniculus</i>)	0.583
126723523	Platelet microbicidal protein 1 precursor (<i>O. cuniculus</i>)	0.582
655841265	Predicted: Trem-like transcript 1 protein (<i>O. cuniculus</i>)	0.573
148224174	UDP-glucuronosyltransferase 1-6 precursor (<i>O. cuniculus</i>)	0.551
126722759	Hemoglobin subunit alpha-1/2 (<i>O. cuniculus</i>)	0.536
655846515	Predicted: Protein S100-A1 (<i>O. cuniculus</i>)	0.516
291409859	Predicted: Protein NipSnap homolog 1 (<i>O. cuniculus</i>)	0.512
291391299	Predicted: cAMP-dependent protein kinase type II-beta regulatory subunit (<i>O. cuniculus</i>)	0.446
655882729	Predicted: Cytochrome b-c1 complex subunit Rieske, mitochondrial (<i>O. cuniculus</i>)	0.431
655850387	Predicted: Peptidyl-prolyl cis-trans isomerase E isoform X1 (<i>O. cuniculus</i>)	0.342
126723706	Haptoglobin precursor (<i>O. cuniculus</i>)	0.309

O. cuniculus: *Oryctolagus cuniculus*; HFD: High fat diet.